Chemosphere 367 (2024) 143559

Contents lists available at ScienceDirect

Chemosphere

journal homepage: www.elsevier.com/locate/chemosphere

Development of an ion exchange process for ammonium removal and recovery from municipal wastewater using a metakaolin K-based geopolymer

C. Maggetti [a], D. Pinelli [a], E. Girometti [a], E. Papa [b], V. Medri [b], E. Landi [b], F. Avolio [c], D. Frascari [a,*]

[a] Department of Civil, Chemical, Environmental and Materials Engineering (DICAM), Alma Mater Studiorum – University of Bologna, via Terracini 28, 40131, Bologna, Italy
[b] National Research Council of Italy, Institute of Science, Technology and Sustainability for Ceramics (CNR-ISSMC former CNR-ISTEC), Via Granarolo 64, 48018, Faenza, RA, Italy
[c] HERA SpA, Direzione Acqua, Viale Carlo Berti Pichat, 2/4, 40127, Bologna, Italy

HIGHLIGHTS

- Geopolymer G13 effectively removed & recovered NH_4^+ from wastewater by ion exchange.
- G13 resulted in high selectivity for NH_4^+ and high operational capacity.
- Performances resulted stable during 7 consecutive adsorption/desorption cycles.
- Empty bed contact time was decreased from 10 to 5 min with no performance reduction.
- Desorption led to product with high fertilizing power (KNO_3 54%$_w$, NH_4NO_3 39%$_w$).

GRAPHICAL ABSTRACT

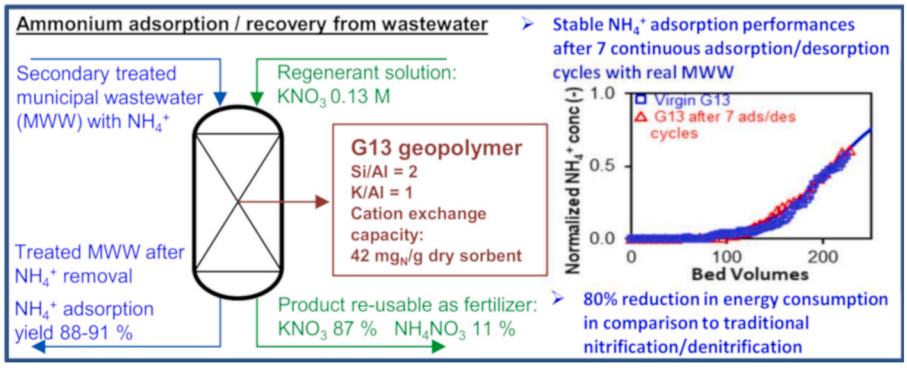

ARTICLE INFO

Handling editor: Xiangru Zhang

Keywords:
Ammonium
Geopolymer
Ion exchange
Nutrient recovery

ABSTRACT

Ion exchange represents a promising process for ammonium removal from municipal wastewater (MWW), in order to recover it for fertilizer production. Previous studies on ammonium ion exchange neglected the assessment of process robustness and the optimization the desorption/recovery step. This study aimed at developing a continuous-flow process of ammonium removal/recovery based on a metakaolin K-based geopolymer, named G13. Process robustness was assessed by operating 7 adsorption/desorption cycles with two types of MWW. These tests resulted in satisfactory and constant performances: operating capacity at 40 $mg_N\ L^{-1}$ in the inlet = 12 $mg_N\ g^{-1}_{dry\ sorbent}$, bed volumes of treated MWW at the selected breakpoint = 199–226, ammonium adsorption

Abbreviations: A_s, asymmetry factor; BT, breakthrough; BP, breakpoint; BV, bed volume; CEC, cation exchange capacity; d_p, particle diameter; EBCT, empty bed contact time; HETP, height equivalent of a theoretical plate; MWW, municipal wastewater; OC, operational capacity; TMWW, treated municipal wastewater; WWTP, wastewater treatment plant.

* Corresponding author. Via Terracini, 28, 40131, Bologna, Italy.
E-mail address: dario.frascari@unibo.it (D. Frascari).

https://doi.org/10.1016/j.chemosphere.2024.143559
Received 28 June 2024; Received in revised form 15 October 2024; Accepted 16 October 2024
Available online 21 October 2024

Pilot plant
Wastewater treatment

yield = 88–91%. Empty bed contact time (EBCT) was decreased from 10 to 5 min without any reduction in performances. The NH_4^+ adsorption process was effectively simulated by the Thomas model, allowing a model-based assessment of the effect of EBCT reductions on process performances. An innovative desorption procedure led to high ammonium recovery yields (86–100%) and to a desorbed product composed primarily of KNO_3 (54%$_w$) and NH_4NO_3 (39%$_w$), two salts largely used in commercial fertilizers. The energy consumption of ammonium removal/recovery with G13 resulted 0.027 kWh $m^{-3}_{treated\ WW}$, with a relevant reduction in comparison to traditional nitrification/denitrification, whereas the operational cost resulted equal to 60–110% of the cost of the benchmark process. These results show that G13 is a promising material to recover ammonium in a circular economy approach.

1. Introduction

Together with phosphorous (P), nitrogen (N) is the main responsible for the eutrophication process. Its accumulation in water bodies causes an excessive proliferation of algae, resulting in a greater bacterial activity and in a lack of oxygen for other aquatic species. Therefore, N must be removed from municipal wastewater (MWW). The most common N removal process is biological nitrification and denitrification (Tchobanoglous et al., 2012; Xiang et al., 2020). On the other hand, N is extensively used as a chemical fertilizer. Most of the N currently produced for agricultural purposes derives from the Haber Bosch process, but its increasing environmental drawbacks are pushing toward other N sources for fertilizer production (Smil Vaclav, 1992). Wastewater (WW) is increasingly considered as a source of water, energy and chemical compounds, mainly fertilizing agents such as nitrogen and phosphorus (Frascari et al., 2018; McCarty et al., 2011; Pinelli et al., 2022a). As nitrification/denitrification requires large tank volumes and a relevant energy consumption, without allowing any N recovery, several other technologies are being developed in a circular economy perspective (Beckinghausen et al., 2020; Ye et al., 2018). N can be chemically precipitated from sludge together with P as struvite, but the market placement of this fertilizer is proving difficult in several countries (Hu et al., 2020; Yu et al., 2012). Another chemical treatment consists in the neutralization of ammonium with HClO to form NCl_3, a very volatile gas. This technique allows the removal of 80–95% of ammonium, but it has high operating costs (Xue et al., 2018). Air-stripping, that requires temperatures >15 °C and chemicals to attain a pH > 9.5 to convert ammonium to ammonia, is generally not applied in large wastewater treatment plants (WWTPs). Membrane separation is characterized by a high operation and maintenance cost, due to the energy required to create a pressure gradient and to the need to frequently replace membranes (Adam et al., 2019).

Adsorption and ion exchange technologies are effective for ammonium (NH_4^+) removal and recovery, in particular when ammonium is present at low concentrations, as in the case of MWW (Medri et al., 2022; Pinelli et al., 2022b). These technologies represent interesting options also for the treatment of the wastewater released in surface water bodies by combined sewer overflows. Natural and synthetic zeolites (Bernal and Lopez-Real, 1993; Hedström, 2001; Kithome et al., 1998; Wang and Peng, 2010), ion exchange polymeric resins (Gefenienė et al., 2006; Jorgensen and Weatherley, 2003, 2006; Vignoli et al., 2015), and polymeric hydrogels (Gefenienė et al., 2006) have been tested for N removal and recovery from MWW. Among them, zeolites are the most promising materials for their high selectivity towards ammonium.

Geopolymers are another group of materials with a high potential for NH_4^+ recovery from MWW. They are synthetic alkali aluminosilicates similar in composition to zeolites, but in amorphous form. They are produced by the reaction of an aluminosilicate powder with an alkali aqueous solution. They are versatile materials with several potential applications in water and wastewater treatment, such as adsorbents/ion-exchangers, carriers for bioreactors, membranes, photocatalysts (Asim et al., 2019; El-Eswed, 2019; Luukkonen et al., 2018; Novais et al., 2017; Rasaki et al., 2019; Siyal et al., 2018). Geopolymers feature high mechanical performances, easy shaping and high reproducibility of the production process (Medri et al., 2020a, 2020b). Mesoporous geopolymers can be produced with interconnected micro--*meso*-macro-ultramacro porosities, leading to a fast diffusion of cations towards the internal porosity (Franchin et al., 2020; Medri et al., 2013; Papa et al., 2015). Several studies investigated the use of geopolymers as cation exchange materials for ammonium removal and recovery (Franchin et al., 2020; Laukkanen et al., 2022; Luukkonen et al., 2016, 2017, 2018, 2019; Sanguanpak et al., 2021; Yu et al., 2023). However, most of these works were conducted with synthetic NH_4^+ solutions, thus neglecting the important matrix effect of a real WW.

In a previous work (Medri et al., 2022) the authors of the current work compared a metakaolin-based geopolymer labelled G13, having a Si/Al ratio equal to 2, a K/Al ratio equal to 1 and K^+ as exchangeable cation (Landi et al., 2013), with an Italian natural zeolite containing mainly chabazite and phillipsite, in terms of NH_4^+ removal and recovery performances. The geopolymer, that outperformed the natural zeolite, was then subjected to an in-depth characterization in terms of mechanical and morphological properties.

G13 was produced by reacting metakaolin with a K silicate solution. The defined stoichiometry and the adopted production process allow to obtain a fully reacted material with high stability, compressive strength over 60 MPa, specific surface area over 50 $m^2\ g^{-1}$ and a well-developed open porosity (Landi et al., 2013; Medri et al., 2022; Papa et al., 2018). Indeed, metakaolin allows the production of reacted and homogeneous geopolymer matrices (Arnoult et al., 2019; Panagiotopoulou et al., 2007). The K/Al molar ratio set to 1 provides sufficient alkali to enable complete charge balancing of the negatively charged tetrahedral aluminum centers, whereas the Si/Al equal to 2 guarantees the formation of small mesopores and a largely homogeneous geopolymer matrix (Davidovits, 2008; Duxson et al., 2005). Furthermore, the use of a potassium silicate as activator enhances the mechanical strength of the geopolymer matrix and as a consequence the robustness of the adsorbent granules (Essaidi et al., 2016). In addition, in the perspective to reuse the product of the NH_4^+ recovery process for fertilizer production, the use of a geopolymer synthetized and periodically regenerated in K^+ form represents an interesting and innovative approach, as K^+ is a crucial component of multi-nutrient NPK fertilizers.

However, it is worth noting that, although the concentrations of solutions commonly used for zeolite regeneration typically exceed 5%, this study examined a solution of KCl with significantly lower concentrations (1%). This choice was informed by findings from Canellas et al. (2019), who demonstrated that KCl exhibits regeneration efficiencies comparable to that of NaCl even at concentrations ten times lower. This reduction in the concentration of the regenerating solution not only allows for a reduction in reagent costs but also yields a desorbed product less concentrated in KCl, making it more suitable for agricultural applications. The main goal of this work was to further develop and optimize the continuous-flow ion exchange process for the removal and recovery of ammonium from treated municipal wastewaters (TMWW) based on the use of the previously developed G13 geopolymer (Landi et al., 2013; Medri et al., 2022). The specific goals of this work and the corresponding novelties were.

a) assessing the process robustness, by means of 7 continuous-flow adsorption/desorption cycles conducted with the same adsorbent charge and with two MWWs, the first being a saline MWW featuring a high competition between ammonium and other cations; conversely, the vast majority of the previous studies of NH_4^+ removal with geopolymers were conducted with synthetic solutions (Franchin et al., 2020; Laukkanen et al., 2022; Luukkonen et al., 2017; Yu et al., 2023), whereas in 1 previous study conducted with a Na-based geopolymer only 3 adsorption/desorption cycles were conducted with actual MWW (Luukkonen et al., 2018);
b) optimizing the adsorption step in terms of empty bed contact time (EBCT); only in 1 previous study relative to NH_4^+ removal using a Na-based geopolymer a preliminary comparison between two EBCTs was performed (Luukkonen et al., 2018), whereas all the other studies on NH_4^+ removal with geopolymers neglected this crucial parameter;
c) performing a simulation of the continuous-flow adsorption step and a model-based investigation of the effect of EBCT reduction on the process performances; to the best of our knowledge, none of the previous studies of NH_4^+ removal with geopolymers included the simulation of the continuous-flow process;
d) further optimizing the desorption process – preliminary developed in a previous study (Medri et al., 2022) - so as to produce a nearly Na-free product potentially useable as raw material for the production of N–K based fertilizers, whereas the previous studies of NH_4^+ recovery from WW generally neglected the issue of the desorbed product valorization for fertilizer production in a circular economy perspective.
e) performing a preliminary assessment of the energy consumption of the proposed process of ammonium removal & recovery, a crucial issue that was generally neglected by the previous studies on NH_4^+ recovery by adsorption or ion exchange.

2. Materials and methods

2.1. Adsorbent characteristics and pre-treatment procedures

The G13 geopolymer, with molar ratios of Si/Al = 2 and K/Al = 1, tested in this work, exhibits sharp edges, smooth fracture surfaces, and a compressive strength of 64.0 ± 6.1 MPa. Its morphology and strength improved after adsorption/desorption cycles due to a fatigue effect. Detailed characteristics and production procedures are in Table S1 and references (Medri et al., 2022; Papa et al., 2022).

2.2. Wastewater and synthetic solution composition

Isotherms and continuous flow tests were conducted with 3 types of solutions and WWs: a) a synthetic solution of NH_4Cl in de-ionized water, used to perform preliminary isotherm tests in the absence of cationic competitors; b) the effluent of a pilot-scale anaerobic membrane bioreactor (AnMBR) that treats the saline MWW of Falconara Marittima (Italy) (Foglia et al., 2020), and c) the effluent of the Bologna (Italy) municipal wastewater treatment plant (WWTP). Both effluents were additioned with NH_4Cl to obtain 40 $mg_N\ L^{-1}$ to mimic the average ammonium content expected in the effluent of a hypothetical WWTP that does not include any nitrogen removal technology. The composition of both effluents is reported in Table S2. As Falconara is a hotspot of seawater intrusion, the Falconara WWTP effluent is characterized by high concentrations of Na^+, K^+, Mg^{2+}, PO_4^{3-} and Cl^-.

2.3. Isotherms

Isotherms were conducted using actual Falconara TMWW and NH_4Cl synthetic solution as detailed in Text S1. The equilibrium N concentration in the solid phase, $C_{S,eq}$ ($mg_N\ g^{-1}_{dry\ sorbent}$), was determined in each test as illustrated in Text S1. Each test was performed in triplicate, with 95% confidence intervals calculated from standard deviation of the mean. Experimental data were interpolated using Langmuir and Freundlich Model equations, according to the best-fit procedures reported in Text S1. Data processing procedures were previously described by Ciavarelli et al. (2012) and Frascari et al. (2019).

2.4. Continuous flow breakthrough tests

Column packing and fluid dynamic characterization. The flow sheet of the laboratory-scale pilot plant used for the continuous-flow adsorption/desorption tests conducted with G13 is reported in Fig. S1. Column packing and fluid dynamic characterization were conducted using a PVC column (total volume 0.144 L, height 1.0 m, inner diameter 21 mm) packed with G13 geopolymer following the Rohm and Hass procedure (Rohm and Hass Company, 2005). The sorbent bed packing quality was assessed using two indicators (Text S2): i) asymmetry factor (As), defined as the ratio of leading to tailing semi-width of the peak at 10% of peak height, and ii) reduced plate height (HETP/d_p), where HETP represents the height equivalent of a theoretical plate and d_p is the average particle diameter. These evaluations were performed as previously described (Pinelli et al., 2016).

Continuous flow adsorption/desorption breakthrough tests. Continuous flow adsorption/desorption breakthrough tests were conducted over seven adsorption/desorption cycles in the column packed with G13 geopolymer: six cycles with saline Falconara TMWW and the last with Bologna TMWW. Operational details are listed in Table 1. Adsorption performance was assessed using four indicators relative to a breakpoint (BP) corresponding to an effluent concentration of 4 $mg_N\ L^{-1}$, detailed in Text S3. Calculations followed methods outlined in prior works (Frascari et al., 2019; Pinelli et al., 2016). Experimental outlet concentrations were fitted using the Thomas Model (Text S4). Desorption/regeneration of the sorbent involved counter-current elution with 2 BVs of de-ionized water to remove suspended solids, followed by 10 BVs of KCl or KNO_3 solution (0.1–0.7 N) to regenerate the sorbent and recover the nitrogen-rich product (Hedström, 2001). Desorption occurred over EBCTs ranging from 20 to 120 min, and performance was quantified by recovery yield (Text S3).

2.5. Analytical methods

Cation analyses were performed with an Integrion ion chromatograph (ThermoFisher Scientific, Walthman, Massachusetts, USA). Details relative to the analytical methods and to the procedure for the assessment of the cation exchange capacity (CEC) of G13 geopolymer are reported in Text S5.

3. Results and discussion

3.1. Adsorption isotherms

Isotherm batch tests were performed with both the NH_4^+ synthetic solution (no cation competition; only 2 points) and the Falconara TMWW (full isotherm in the 10–380 $mg_N\ L^{-1}$ range). The isotherm with Falconara TMWW was conducted both with virgin G13 and with the G13 unpacked from the column after the 7 adsorption/desorption cycles, in order assess possible changes in adsorption performance. The results of the isotherm tests are shown in Fig. 1 in terms of experimental data and best-fitting simulations.

In agreement with the results of previous experiments conducted only on virgin G13 (Medri et al., 2022), the isotherms resulted favourable. In the two tests conducted with the NH_4Cl synthetic solution (blue triangles, no competition from other cations), the NH_4^+ sorbed concentrations showed minor deviations in comparison with the values obtained with the real TMWW, suggesting that G13 has a very high selectivity towards NH_4^+ and a low affinity towards Na^+, whose concentration in the Falconara saline TMWW is 5 times higher than that of

Table 1
Operating conditions and performances of the breakthrough tests conducted with geopolymer G13 in the 0.60-m column. The inlet NH_4^+ concentration was equal to 40 ± 1 $mg_N\ L^{-1}$.

Operational conditions	Test ID[a]	FA-10a	FA-10b	FA-10c	FA-10d	FA-7.5	FA-5	BO-10
	EBCT, adsorption (min)	10	10	10	10	7.5	5.0	10
	Sup. Velocity, adsorption (m/h)	3.60	3.60	3.60	3.60	4.80	7.20	3.60
	EBCT, desorption (min)	60	120	20	20	20	20	20
	Sup. Velocity, desorption (m/h)	0.60	0.30	1.80	1.80	1.80	1.80	1.80
	Regenerant, type and conc.	KCl 0.13 N	KCl 0.13 N	KCl 0.13 N	KCl/KNO_3[b]	KNO_3 0.13 N	KNO_3 0.67 N	KCl/KNO_3[b]
Performances	Bed volumes treated @BP[c]	208	215	226	199	202	190	199
	NH_4^+ adsorption yield @ BP[c]	91%	90%	88%	90%	90%	91%	91%
	Sorbent utilization efficiency @ BP[c]	72%	87%	92%	87%	87%	82%	89%
	Overall NH_4^+ recovery yield @ BP[c]	98%	100%	95%	100%	98%	90%	86%
	NH_4^+ conc. in the desorbed product ($mg_N\ L^{-1}$)[d]	754	572	479	1029	767	923	1318
	Bed volumes of the second desorption fraction[d]	11	14	13	9	8	6	5
	NH_4NO_3 mass fraction in the desorbed product[d]	e	e	e	11%	39%	8%	16%
	$NaNO_3$ mass fraction in the desorbed product[d]	e	e	e	0.3%	0.7%	0.5%	0.3%
	KNO_3 mass fraction in the desorbed product[d]	e	e	e	87%	54%	88%	80%
NH_4^+ OC[f]	@ $C_{L0,N}$, from BT test[g]	12.3	11.8	10.6	11.7	12.1	12.9	11.9
	@ BP of the BT test[h]	11.0	10.3	9.7	10.2	10.6	10.6	10.7

[a] BO = Bologna WWTP effluent; FA = Falconara AnMBR effluent; the number indicates the EBCT applied during the adsorption step, expressed in minutes.
[b] The first 5 BVs were conducted with KCl 0.13 N, the following BVs with KNO_3 0.67 N.
[c] All the performance parameters were evaluated at a breakpoint corresponding to an average NH_4^+ concentration in the treated effluent equal to 4 $mg_N\ L^{-1}$.
[d] Data referred to the second fraction of the fractionated desorption (the valuable product).
[e] NO_3 was not used as desorption agent in these tests.
[f] NH_4^+operating capacity estimated from the breakthrough tests.
[g] NH_4^+operating capacity ($mg_N\ g_{dry\ sorbent}^{-1}$) estimated at saturation in each breakthrough test; for the tests stopped before saturation, the estimate is based on the best fitting Thomas curve, extrapolated until resin saturation.
[h] NH_4^+operating capacity ($mg_N\ g_{dry\ sorbent}^{-1}$) estimated in each breakthrough test at the selected breakpoint (average NH_4^+concentration in the treated effluent equal to 4 $mg_N\ L^{-1}$).

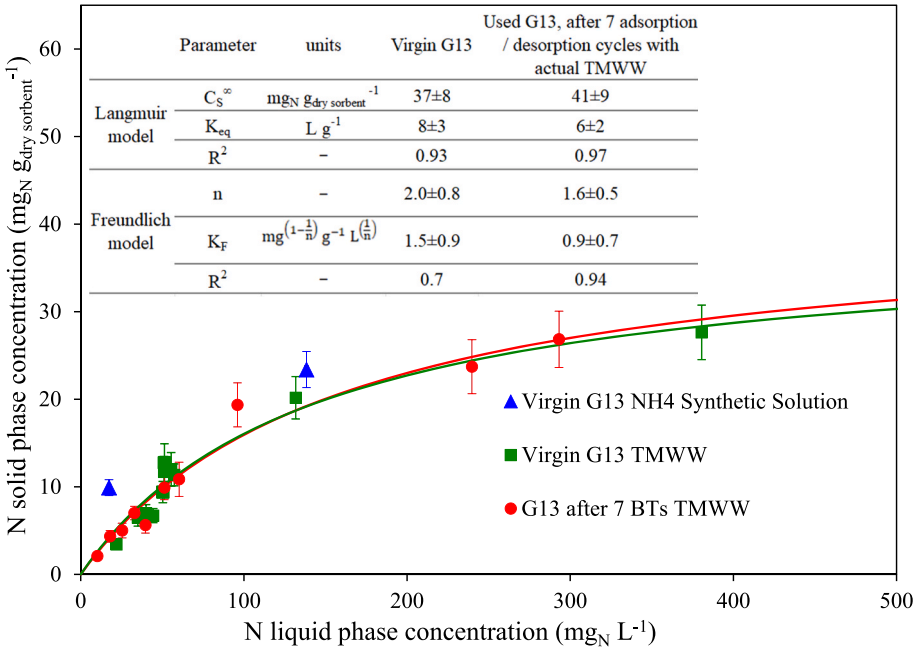

Fig. 1. Isotherms conducted with geopolymer G13, with the NH_4Cl synthetic solution and with the Falconara TMWW, before and after the operation of 7 adsorption/desorption cycles. Continuous lines correspond to the best-fitting simulations performed with the Langmuir model, relatively to the experimental data obtained with virgin G13 + Falconara TMWW (green line) and used G13 + Falconara TMWW (red line). Best-fitting model parameters ±95% confidence intervals, relative to the interpolation with the Freundlich and Langmuir models of the isotherms conducted with virgin G13 and with the used material after 7 adsorption/desorption cycles, are reported in the top-part of the Figure. (For interpretation of the references to colour in this figure legend, the reader is referred to the Web version of this article.)

the spiked NH_4^+. In the perspective to use the desorbed product as a secondary raw material for fertilizer production, the selection of a sorbent with a low affinity for Na^+ is crucial, as Na^+ is toxic for several crops and it damages soil texture.

The experimental data of the two isotherms conducted with virgin and used G13 were interpolated with the Langmuir and Freundlich models. As shown in Fig. 1, in both cases, the Langmuir model resulted the best-fitting one. The observation of Fig. 1, in agreement with a statistical analysis of the Langmuir best-fit parameters relative to the 2 complete isotherms, indicates that the operation of 7 consecutive adsorption/desorption cycles with actual TMWW did not lead to statistically significant variations in ammonium adsorption performances of G13. This represents an important result in the perspective to re-use each load of sorbent for a very high number of cycles.

The sorbed NH_4^+ concentrations estimated by means of the Langmuir model in equilibrium with an infinite liquid-phase concentration (C_S^∞, 37–41 $mg_N\ g_{dry\ sorbent}^{-1}$) are in good agreement with the G13 CEC estimated through an independent approach (42 $mg_N\ g_{dry\ sorbent}^{-1}$; Table S1 and Text S5).

The results show that geopolymer G13 outperforms zeolites in studies of ammonium adsorption. For example, in studies of NH_4^+ removal from groundwater or tap water conducted with Clinoptilolite or zeolites synthetized from volcanic ash, the sorbed concentrations in equilibrium with 40 $mg_N\ L^{-1}$ in the liquid resulted equal to 3.5–4.0 $mg_N\ g_{dry\ sorbent}^{-1}$, versus 9 $mg_N\ g_{dry\ sorbent}^{-1}$ for G13 in tests conducted with a saline WWTP effluent in this work (Gagliano et al., 2022; Vocciante et al., 2018). Conversely, the G13 performances obtained in this work are comparable to those obtained in other studies of NH_4^+ adsorption with geopolymers (Luukkonen et al., 2018; Sanguanpak et al., 2021; Yu et al., 2023).

3.2. Continuous flow breakthrough tests

Fluid-dynamic column characterization. Before performing the breakthrough tests, a fluid-dynamic analysis was performed on the adsorption column, by means of tracer tests conducted at the three EBCTs applied in the continuous adsorption tests: 10, 7.5 and 5 min. This analysis showed a good quality of the adsorption bed packing, without any relevant preferential pathways. The average asymmetry factor *As* resulted equal to 1.5 ± 0.2, whereas $HETP/d_p$ was equal to 19 ± 7. Further tests indicated that these packing quality parameters resulted stable during the 7 adsorption/desorption cycles. This result represents a further indication of the robustness of the tested G13 geopolymer.

Continuous flow breakthrough tests. Initially, 4 repeated adsorption breakthrough tests (FA-10a, FA-10b, FA-10c, FA-10d) were conducted with Falconara TMWW, to investigate the selectivity of the tested geopolymer towards NH_4^+ in continuous mode and the robustness of the G13 geopolymer. An EBCT of 10 min was selected; this value represents the lower limit of the EBCT range used in the majority of previous studies relative to NH_4^+ removal with natural and synthetic zeolites (Hedström, 2001). The G13 bed was regenerated after each adsorption test, according to the operational conditions reported in Table 1. The breakthrough curves for NH_4^+, Na^+, Mg^{2+} and Ca^{2+} relative to test FA-10d are shown in Fig. 2.

The first cation to be eluted was Na^+, followed by Mg^{2+} and Ca^{2+}, whereas NH_4^+ was the last cation to be eluted. In agreement with preliminary results presented previously (Medri et al., 2022), these data confirm the high selectivity of G13 towards NH_4^+ versus the other wastewater cations, especially sodium which needs to be eliminated form the final product to allow its use for fertilizer production. The Mg^{2+} breakthrough curve exhibits a peak that surpasses the expected value of 1 for $C_L/C_{L,0}$, due to competitive adsorption between Mg^{2+} and the other cations. Indeed, as a result of the higher affinity of G13 for NH_4^+ and Ca^{2+} in comparison to Mg^{2+}, during the Mg^{2+} breakthrough that starts at 40 BVs, the packed bed exchanges a fraction of the previously sorbed Mg^{2+} with incoming NH_4^+ and Ca^{2+}. As the desorbed Mg^{2+} adds up to the one entering in the column, between 80 and 140 BVs the Mg^{2+} concentration in the column outlet results higher than the entering value ($C_L/C_{L,0} > 1$).

As detailed in Table S3, the average effluent concentration at breakpoint falls within the limits established by the World Health Organization (World Health Organization, 2006) for the safe reuse of wastewater for agricultural irrigation purposes. Specifically, as a result of the high Na^+ and Cl^- concentrations, the treated effluent falls under the category with a slight to moderate degree of restriction on use, which allows for the irrigation of crops not intended for direct human consumption.

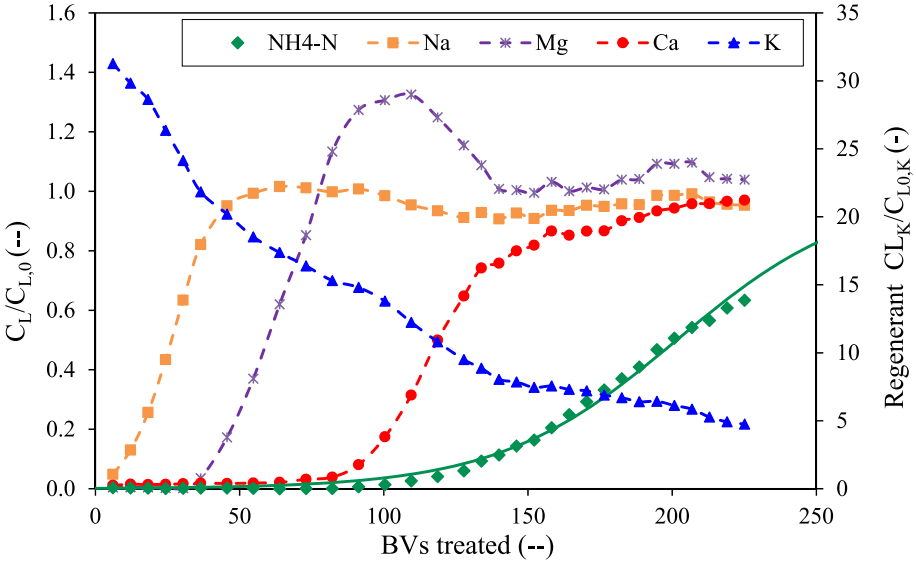

Fig. 2. Breakthrough test FA-10d with geopolymer G13 in K^+ form, conducted with Falconara TMWW. EBCT = 10 min, feed NH_4^+ concentration = 40 $mg_N\ L^{-1}$. The best fit of the NH_4^+ breakthrough curve with the Thomas model is shown as a continuous green line. The concentrations of all ions exiting the column have been normalized to their respective concentrations in the influent $C_L/C_{L,0}$, ($C_{L,0\ Na^+} = 214 \pm 7$ mg L^{-1}, $C_{L,0\ K^+} = 24 \pm 3$ mg L^{-1}, $C_{L,0\ Mg^{2+}} = 32 \pm 7$ mg L^{-1}, and $C_{L,0\ Ca^{2+}} = 97 \pm 9$ mg L^{-1}). Normalization of the outlet concentrations has been performed to bring all data onto the same scale, enhancing the visual clarity of the figure, considering that the inlet concentration values span different orders of magnitude. (For interpretation of the references to colour in this figure legend, the reader is referred to the Web version of this article.)

The NH_4^+ breakthrough curves relative to all the 7 adsorption tests are reported in Fig. S2. Its observation, in agreement with the process performances reported in Table 1, indicates that the NH_4^+ recovery process conducted with G13 resulted stable during 4 repeated adsorption/desorption cycles.

Two further tests were dedicated to decrease and optimize the EBCT of the adsorption step. They were performed at EBCTs of 7.5 min (FA-7.5) and 5 min (FA-5), using Falconara TMWW. As shown in Fig. S2, where the NH_4^+ BT curves at the three tested EBCTs are reported, and in Table 1, the adsorption performanes were not significantyl affected by the EBCT reduction. The EBCT was selected as a key parameter to optimize the fixed-bed adsorption processes due to its direct impact on the interaction time between cations and the adsorbent material. Indeed, as the EBCT is equal to V_{bed}/flow rate, any decrease in EBCT determines a corresponding decrease of the column volume, resulting in a lower investment cost. On the other hand, relevant EBCT decreases can determine mass-transfer limitations in the adsorption process, leading to a premature breakthrough curve. This would lead to a less efficient utilization of the sorbent bed, resulting in a higher operational cost for the periodic sorbent replacement (Frascari et al., 2016). Therefore, the EBCT fine tuning represents a key step in the overall optimization of the adsorption process.

To further investigate the process robustness, a different TMWW was used in the last test, BO-10, conducted at a 10-min EBCT with the effluent of the Bologna (Italy) full scale municipal WWTP (Table S2). As shown in Table 1 and Fig. S2, no statistically significant differences were detected between the results of this test and those of the analogous tests conducted with Falconara WWTP effluent (FA-10a, FA-10b, FA-10c, FA-10d). This represents an important result, in the perspective to use the G13 geopolymer for NH_4^+ removal from WWs with different compositions.

The Thomas model (Text S4) was used to interpolate the experimental NH_4^+ adsorption profiles relative to all the breakthrough tests. As shown in Fig. S2, the fitting was always good ($R^2 = 0.973–0.990$). The analysis of the best-fitting parameters K_{Th} and $C_{s,eq}$, reported in Table S4, indicates a linear trend of slowly decreasing K_{Th} with increasing EBCT: K_{Th} [L h^{-1} mg^{-1}] = 0.00946–0.000492 • EBCT [min]; $R^2 = 0.801$. This K_{Th} – EBCT relationship, together with the average $C_{s,eq}$ obtained in the 7 experimental tests ($C_{s,eq,average}$ = 12.0 mg_N $g_{dry\ resin}^{-1}$), was used to test the Thomas model capability to predict the process performance at EBCTs lower than those experimentally tested. As an example, the predicted curve corresponding to a 3-min EBCT is reported in Fig. S2. The observation of Fig. S2, together with an analysis of the adsorption performances reported in Table 1 (BVs treated @BP, NH_4^+ adsorption yield @ BP), indicates that the decrease in EBCT from 10 to 5 min did not lead to any significant variation in process performance, whereas the further EBCT reduction to 3 min determined an appreciable decrease in performance. The measured pressure drops across the 60 cm column varied between 0.03 and 0.07 bar/m, in good agreement with the corresponding values estimated by means of the Ergun equation, assuming an average diameter of the particles equal to 533 μm (average value in the 355–710 μm range; Table S1) and a 0.39 effective porosity.

These results show that G13 allowed the achievement of high and stable ammonium removal performances over 7 consecutive adsorption/desorption cycles performed with real WWs of different salinity, at different EBCTs varying between 5 and 10 min. This outcome is considered a relevant progress towards the development of an ammonium removal & recovery technology characterized by low operational expenditures, thanks to the potential to re-use G13 over a high number of cycles, and low capital cost, thanks to the reduction in column size connected to the decrease in EBCT.

These results are of particular interests if compared to previous continuous-flow studies of ammonium removal from MWW. Most previous studies used EBCTs in the 10–30 min range (Jorgensen and Weatherley, 2006; Langwaldt, 2008). In the attempt to descrease the EBCT, in a study of ammonium removal from a synthetic WW conducted with a zeolite synthetized from vlocanic ash, the EBCT reduction from 8 to 4 min determined in synthetic solution tests a 3-fold decrease in the time corresponding to the 10% breakpoint (Gagliano et al., 2022); in the same study, a 3-fold decrease in performances was observed after just 1 regeneration step. In an investigation of ammonium removal from MWW with an Na-based geopolymer, the EBCT reduction from 6 to 3 min led to a drastic reduction in the time for attainment of the 50% breakpoint; in addition, during 3 consecutive adsorption/desorption cycles the geopolymer regeneration conducted with 0.1 M NaOH and 0.2 M NaCl determined a 30–50% decrease in ammonium removal (Luukkonen et al., 2018). In a study of NH_4^+ removal from a synthetic solution conducted with a geopolymer obtained through a combined granulation–alkali activation–direct foaming process, the 50% breakpoint was obtained after just 9–17 BVs, versus 200–220 BVs in this work (Yu et al., 2023). Franchin et al. (2020), in a study of NH_4^+ removal from a synthetic solution conducted with geopolymers fabricated via additive manufacturing, observed a relevant decrease in NH_4^+ removal efficiency when the EBCT was decreased from 19 to 10 min.

3.3. Total and operating capacity of the K-based G13 geopolymer

The BT tests were used to obtain an overall estimate of the NH_4^+ operating capacity (OC) of G13 evaluated – in the presence of competing cations – at different points of the BT curve. The OC data are shown in the last 2 rows of Table 1. The first estimate (OC @ $C_{L0,N}$, from BT test) represents the ammonium OC estimated at resin saturation, when all the sorbent is in equilibrium with the feed. This estimate corresponds to parameter $C_{s,eq}$ in the Thomas model (Text S4 and Table S4), and the average value resulted equal to 12.0 ± 0.7 mg_N $g_{dry\ sorbent}^{-1}$. The second estimate (OC @ BP) represents the OC evaluated at the selected BP (average NH_4^+ concentration in the treated effluent equal to 4 mg_N L^{-1}). The average value resulted equal to 10.4 ± 0.4 mg_N $g_{dry\ sorbent}^{-1}$. As expected, the OC estimated at the BP is lower than that estimated at saturation, as at the BP not all the sorbent sites are used (mean resin utilization efficiency = 84 ± 7%). The average values of both OC estimates have very small confidence intervals (3.8–5.8% of the average values), which represents a further confirmation of the stability and robustness of the tested sorbent during the 7 adsorption/desorption cycles. Both OC estimates are significantly lower than the CEC evaluated through a dedicated test using a synthetic solution (42 ± 8 mg_N $g_{dry\ sorbent}$ $^{-1}$; Table S1). This shows that, even though the G13 selectivity towards ammonium is very high, the relatively low ammonium concentration in the TMWW and the presence of competing cations exert a substantial impact on the sorbent performance.

The total capacity of geopolymer G13 (CEC; 42 ± 8 mg_N $g_{dry\ sorbent}$ $^{-1}$) is higher than most literature values relative to zeolites and geopolymers. The CECs reported in previous investigations varied in the 10–18 mg_N $g_{dry\ sorbent}^{-1}$ range in tests of NH_4^+ removal from tap water conducted with zeolites synthetized from volcanic ash (Gagliano et al., 2022), and in the 18–29 mg_N $g_{dry\ sorbent}^{-1}$ range in tests of NH_4^+ removal from MWW conducted with an Na-based geopolymer (Luukkonen et al., 2018). Franchin et al. (2020) report, for 3D-printed metakaolin-based geopolymers with Si/Al = 1.9 and Na/Al = 1.0, a 2.6 mg_N $g_{dry\ sorbent}$ $^{-1}$ CEC and an 80% removal efficiency in a NH_4^+ synthetic solution. Hedström (2001) reported CECs between 14 and 32 mg_N $g_{dry\ sorbent}^{-1}$ for zeolites. Langwaldt (2008) reported 12–19 mg_N $g_{dry\ sorbent}^{-1}$ for 7 Clinoptilolites. A 33 mg_N $g_{dry\ sorbent}^{-1}$ CEC was obtained in tests of NH_4^+ removal from MWW with a natural Italian zeolite composed of a mixture of Chabazite and Phillipsite (Pinelli et al., 2022b). Conversely, CECs higher than those obtained in this study for G13 were reported by Guida et al. (2020) for synthetic and engineered zeolites (up to 60 mg_N $g_{dry\ sorbent}$ $^{-1}$), and by Yu et al. (2023) thanks to the progressive aging of geopolymers with different Ca contents (up to 87 mg_N $g_{dry\ sorbent}^{-1}$).

With regard to operating capacity, the average value measured for G13 in the presence of competing cations in equilibrium with 40 mg_N L^{-1} (12 mg_N $g_{dry\ sorbent}^{-1}$) is higher than the typical values reported under

similar conditions for different zeolites: 1–7 $mg_N\ g^{-1}_{dry\ sorbent}$ according to Hedström (2001); 0.4–0.8 $mg_N\ g^{-1}_{dry\ sorbent}$ measured by Guida et al. (2020); 6.5 $mg_N\ g^{-1}_{dry\ sorbent}$ obtained with a Chabazite/Phillipsite natural mixture (Pinelli et al., 2022b). Slightly higher values were obtained by Guida et al. (2021) for an engineered Zeolite-N (15–17 $mg_N\ g^{-1}_{dry\ sorbent}$) in correspondence of an ammonium concentration in the 1–26 $mg_N\ L^{-1}$ range.

3.4. Optimization of the desorption/regeneration phase

The next step consisted in the optimization of the desorption step in terms of EBCT and nature of the desorbing solution. In the first 3 repeated tests (FA-10a, FA-10b and FA-10c), a 0.13 N (10 g L^{-1}) KCl solution was used as regenerant, with a desorption phase EBCT varying between 20 and 120 min. The desorption curves of NH_4^+, Na^+, Mg^{2+} and Ca^{2+} obtained in FA-10a, as well as the trend relative to the desorbing cation K^+, are shown in Fig. S3. The comparison between the desorbed NH_4^+ curves at different EBCTs is shown in Fig. S4. The NH_4^+ recovery evaluated at the BP was very high (95–100% in the first 3 tests; Table 1) and no appreciable differences were noted by changing the desorption EBCT. Thus, a 20 min EBCT was adopted for the subsequent desorption tests.

Fig. S3 shows that the strong affinity of G13 for ammonium delays its desorption. This provides the chance to perform a fractionated desorption of ammonium. Indeed, as initially proposed in a previous study of the same research group (Medri et al., 2022), two separated fractions could be collected: a first one, including the first 4 BVs, rich in Na^+, and a second one, from the 5th to the 16th BV, characterized by a high ammonium concentration (479–754 $mg_N\ L^{-1}$ in the 1st 3 tests) and a very low Na^+ content (16–60 mg L^{-1}), leading to a total amount of desorbed solution equal to 16 BVs. The first fraction represents a waste stream, associated to a minor loss in N (N lost in the first fraction = 9% of the total N desorbed). As for the second fraction, in order to turn it into an interesting product for the fertilizer industry, in tests FA-7.5 and FA-5, KCl was replaced by KNO_3, so as to eliminate from the final product Cl^-, toxic for several crops, and replace it with NO_3^-, a widespread fertilizer.

Thus, in FA-7.5 desorption was performed at a 20-min EBCT using a 0.13 N KNO_3 solution. As expected, the desorption performances were equivalent to those of KCl (Table 1). The use of the KNO_3 solution led to an interesting desorbed product, composed mainly of KNO_3 (54%$_w$) and NH_4NO_3 (39%$_w$), two salts with a high fertilizing power, whereas the $NaNO_3$ mass fraction was reduced to just 0.7% (data referred to the 2nd desorbed fraction).

Then, in test FA-5 the KNO_3 concentration was increased to 0.67 N to reduce the BVs – and therefore the amount of water to be evaporated for the production of a concentrated fertilizer – needed to desorb N. The positive effect of the reduction of the BVs required to desorb 95% of the N (17 ± 1 on average for tests FA-10a, FA-10b and FA-10c) to 11.6 (FA-5) was thwarted by the overlapping of all the cation desorption curves, which led to a fractionated product characterized by a significantly lower NH_4NO_3 mass fraction (Table 1).

To further optimize the process, a 2-step desorption was attempted in test FA-10d (Fig. 3): at first, 5.3 BVs of KCl 0.13 N were supplied to slowly desorb Na^+, thus minimizing NH_4^+ loss in the first fraction; then 6.3 BVs of 0.67 N KNO_3 were eluted to rapidly recover most of the NH_4^+. The choice of KCl instead of KNO_3 as desorption solvent for the first fraction (waste) is due to the considerably lower market price of KCl in comparison to KNO_3. This approach led to a recovered product (2nd fraction) slightly more interesting than that obtained in FA-5 (NH_4NO_3 11%, KNO_3 87%, $NaNO_3$ 0.3%). A complete cost-benefit analysis is in progress, considering all the investment and operational costs, in order to find the optimal desorption strategy. Furthermore, the first 5 BVs, which are discarded, along with the 2 BVs used to rinse the column between the adsorption and desorption steps, are recycled and recirculated to the head of the plant. This recycling approach helps in reducing waste and optimizing resource usage, thereby contributing to the overall efficiency and sustainability of the process.

On the basis of the results of the ammonium adsorption/desorption tests, the following optimized condition was identified: adsorption EBCT 7.5 min (average value in the 5–10 min range tested experimentally); 4 $mg_N\ L^{-1}$ adsorption breakpoint achieved after 202 BVs (Table 1); desorption performed with 0.13 N KNO_3 (solution density 1014 kg m^{-3}) at 20 min EBCT; number of BVs required to complete the desorption step = 16 (section 3.4), corresponding to a ratio of (desorption solution)/(treated WW) = 16/202 = 0.0792 $m^3\ m^{-3}$.

An additional adsorption/desorption test was aimed at investigating the interaction of G13 with other cations – in particular heavy metals – present in the tested WWTP effluents, with emphasis on the potential consequences on the use of the desorbed product as a fertilizer. The test, conducted with Bologna WWTP effluent, focused on the 3 heavy metals present at higher concentrations in this effluent, i.e. Zn (0.038 mg L^{-1}),

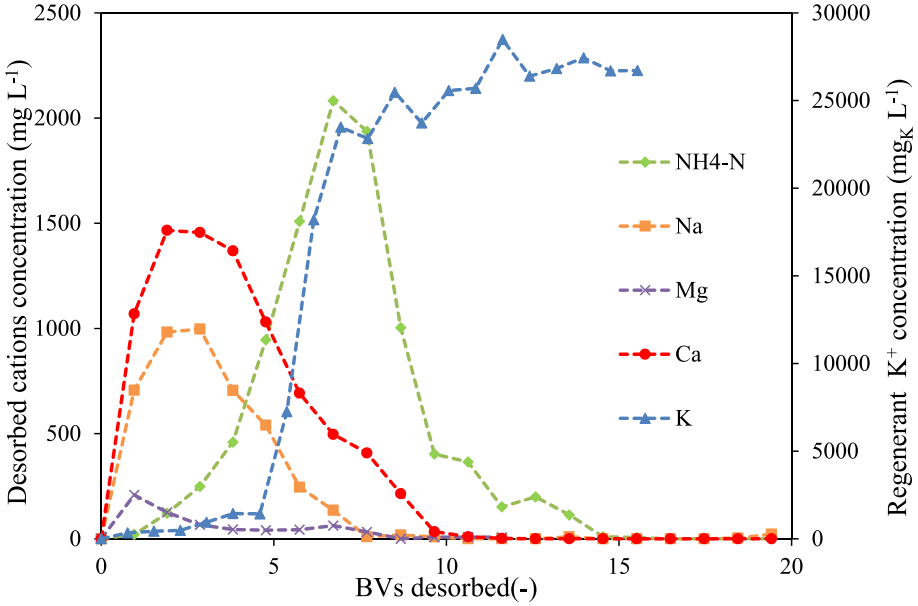

Fig. 3. Cation desorption breakthrough curves in test FA-10d: desorption conducted with KCl 0.13 N for the first 5 BVs and then with KNO_3 0.76 N, at a 20 min EBCT.

Cu (0.0071 mg L^{-1}) and Ni (0.017 mg L^{-1}). The test resulted in average removals during the adsorption step equal to 76% (Zn), 86% (Cu) and 50% (Ni). As the desorption yields varied in the 80–90% range, the concentrations in the desorbed product, divided by the total desorbed solids, resulted equal to 23–26 mg $kg^{-1}_{dry\ matter}$ (Zn), 4.9–5.6 mg $kg^{-1}_{dry\ matter}$ (Cu) and 6.9–7.7 mg $kg^{-1}_{dry\ matter}$ (Ni). These concentrations vary between 3% and 15% of the strictest limits imposed by the 2019/1009 EU regulation on fertilizers (500 mg $kg^{-1}_{dry\ matter}$ for Zn, 200 mg $kg^{-1}_{dry\ matter}$ for Cu, 50 mg $kg^{-1}_{dry\ matter}$ for Ni) (European Commission, 2019). These results indicate that the proposed process of NH_4^+ removal with G13 leads to the additional benefit of medium-to-high removals of the main heavy metals detected in WWTP effluents, while the obtained concentrations in the desorbed product do not hinder its potential use for fertilizer production.

3.5. Preliminary assessment of the energy consumption and operational cost of the process of ammonium recovery

The preliminary assessment of the energy consumption, operational cost and land occupation of the proposed technology of ammonium removal/recovery by ion exchange was based on the optimal condition illustrated in section 3.4. The height of the packed bed of a hypothetical full-scale column was assumed equal to 2.5 m, a reasonable value considering that the height of adsorption columns in the field of water treatment is typically <3 m. Therefore, assuming as scale-up criterion to maintain the 7.5-min adsorption EBCT and the 20-min desorption EBCT, the superficial velocities resulted equal to 20 m h^{-1} and 7.5 m h^{-1}, respectively. Since the process operational cost depends strongly on the number of adsorption/desorption cycles (N_{cycles}) that can be performed with one G13 load, on the basis of feedback received from manufacturers of ion exchange resins, two scenarios were considered, corresponding to $N_{cycles} = 200$ and $N_{cycles} = 500$.

On the basis of the methodology illustrated in detail in Text S6, Supplementary Materials, the operational cost of the proposed process resulted to be given by the following items: electricity for adsorption/desorption, 0.005 € $m^{-3}_{treated\ MWW}$ (0.027 kWh $m^{-3}_{treated\ MWW}$); G13 purchase + disposal of the spent G13, 0.009–0.021 € $m^{-3}_{treated\ MWW}$ (for N_{cycles} varying in the 200–500 range). Thus, the total operational cost of ammonium removal/recovery resulted variable in the 0.013–0.026 € $m^{-3}_{treated\ MWW}$ range. In the best-case scenario of $N_{cycles} = 500$, this cost is 40% lower than the operational cost of the benchmark nitrification/denitrification process, estimated at 0.023 € $m^{-3}_{treated\ MWW}$ (Text S7, Supplementary Material) (Kroiss and Cao, 2014). Conversely, in the conservative scenario of $N_{cycles} = 200$, the ion-exchange process slightly exceeds the benchmark process. In addition, the energy consumption of the benchmark technology, estimated at 0.137 kWh $m^{-3}_{treated\ MWW}$ (Text S7), is 5 times higher than that of the proposed ion exchange technology. For a complete evaluation of the operational cost of the ammonium removal/recovery process with G13, one should consider that the fractionated desorption step – fed with a largely used fertilizer such as KNO_3 - produces in turn a fertilizer composed mainly of KNO_3 (54%w) and NH_4NO_3 (39%w), which could find a suitable market placement. As the assessment of the potential selling price of this product and of the pre-treatments that it could require goes beyond the scope of this work, this preliminary evaluation of the operational cost of ammonium removal/recovery included neither the purchase of KNO_3 nor the revenues deriving from the sale of the final product.

The comparison between ion exchange and the benchmark technology was extended to the assessment of the amount of land required, a crucial factor in several WWTPs. Taking a reference MWW flow rate of 1000 $m^3\ h^{-1}$, in the above-described optimized condition the ion exchange process requires 10 adsorption columns in parallel, each with a 2.5-m diameter and a 2.5-m height, for a total land occupation of 50 m^2. Considering that the continuous-flow operation requires the presence of 10 additional desorption columns, and adding an extra 100% surface for pumps, piping and instrumentation, the total land occupation is equal to about 200 m^2. Conversely, considering a typical MWW with BOD_5 = 220 mg L^{-1} and N–NH_4 = 40 mg L^{-1}, according to the methodology illustrated in Text S7, at a winter temperature of 12 °C the land occupation is equal to 56 m^2 for an activated sludge process aimed only at BOD removal, and to 1374 m^2 for a nitrification/denitrification activated sludge process aimed at removing both BOD and N. Thus, the additional land required for N removal, equal to about 1320 m^2, is roughly 6 times the land required by the ion exchange N-removal process.

3.6. Further research needs towards full scale application

The results of the continuous-flow laboratory-scale tests indicate that G13 is a very promising material for NH_4^+ removal/recovery from MWW. The proposed technology could find different applications: i) NH_4^+ removal/recovery in WWTPs not equipped with biological nitrification/denitrification, a frequent situation in developing countries; ii) further reduction of NH_4^+ effluent concentrations in WWTPs already equipped with biological nitrification/denitrification, if requested by new regulations; for example, the revised Wastewater Treatment Directive approved by the EU Parliament in April 2024 reduced the limit for WWTP discharges from 10 to 8 $mg_N\ L^{-1}$ for WWTPs serving >150000 people equivalent; iii) NH_4^+ removal/recovery from the floating fraction obtained by municipal sludge centrifugation, a waste typically containing 600–800 $mg_N\ L^{-1}$.

In the perspective of attaining full-scale applications, further research is needed in order to: i) assessing the maximum number of adsorption/desorption cycles attainable with one load of G13; ii) optimizing the desorption step in terms of EBCT and salt concentration; iii) developing a model of multi-component cation adsorption/desorption, for the design of the full-scale process; iv) identifying and demonstrating the most effective technology to obtain a marketable fertilizer from the desorbed product; v) developing a complete cost/benefit analysis and LCA of the process.

4. Conclusions

Geopolymer G13 has proven to be a promising material for NH_4^+ removal and recovery from MWW, with a high operational capacity (12.0 $mg_N\ g^{-1}_{dry\ sorbent}$) and a significant amount of MWW treated at the 4 $mg_N\ L^{-1}$ breakpoint (199–226 BVs), showing excellent selectivity towards ammonium. The NH_4^+ adsorption/desorption performances, as well as the material's mechanical properties remained stable during 7 adsorption/desorption cycles conducted with two different MWWs, one of which had high salinity. In the attempt to optimize the adsorption step, the EBCT was gradually reduced from 10 to 5 min, without any relevant variation in process performances. The Thomas model led to a satisfactory simulation of the NH_4^+ adsorption process, enabling model-based predictions of the effects of further EBCT reductions on the adsorption performances. An innovative fractioned desorption procedure, based on the integration of KCl and KNO_3 as desorption solvents, allowed the obtainment of high ammonium recovery yields (86 ÷ 100%) and of an interesting desorbed product composed mainly of KNO_3 (54% w) and NH_4NO_3 (39%w), two salts with a high fertilizing power, whereas the content of Na^+ – toxic for several crops and harmful for soils – was minimized. On the basis of a preliminary assessment, compared to the traditional nitrification/denitrification process, the proposed process of ammonium removal/recovery with G13 allows to achieve a relevant reduction in both energy consumption and land occupation. Lastly, the operational cost of the proposed technology varies between 60% and 110% of the cost of the benchmark process, depending on the number of adsorption/desorption cycles attainable with each load of G13.

CRediT authorship contribution statement

C. Maggetti: Writing – review & editing, Writing – original draft, Investigation, Data curation, Conceptualization. **D. Pinelli:** Writing – review & editing, Writing – original draft, Supervision, Methodology, Conceptualization. **E. Girometti:** Investigation. **E. Papa:** Investigation. **V. Medri:** Investigation. **E. Landi:** Investigation. **F. Avolio:** Validation, Funding acquisition. **D. Frascari:** Writing – review & editing, Supervision, Project administration, Funding acquisition, Conceptualization.

Declaration of competing interest

The authors declare that they have no known competing financial interests or personal relationships that could have appeared to influence the work reported in this paper.

Acknowledgments

This work received funding from the European Union's Horizon Europe research and innovation program under grant agreement No 101082048 (MAR2PROTECT project) and from the MUR PRIN 2022 grant No 20229THRM2 (GEA project) funded by the European Union – Next Generation EU.

Abbreviations

As	Asymmetry factor
BP	Breakpoint
BT	Breakthrough test
BV	Empty bed volume of sorbent (mL)
BVs	Number of bed volumes
C_L	Liquid phase concentration of ions (mg L^{-1})
$C_{L,0}$, $C_{L,eq}$	Initial and final (equilibrium) ion concentration in the liquid phase (mg L^{-1})
$C_{S,eq}$	Final (equilibrium) NH_4–N concentration in the solid phase (sorbent) during the isotherm tests ($mg_N\ g^{-1}_{dry\ sorbent}$)
$C^{\infty}_{S,i}$	Maximum amount of *i*-compound sorbed per unit mass of adsorbent, in the Langmuir model (mg $g^{-1}_{dry\ sorbent}$)
EBCT	Empty bed contact time, ratio between resin bed volume (L) and flowrate (L h^{-1}) used in the breakthrough test (min)
HETP	Height equivalent to a theoretical plate
$K_{eq,i}$	Equilibrium constat related to the affinity between the binding sites and the *i*-compound, in the Langmuir model (L mg_i^{-1})
$K_{F,i}$	Sorption capacity in the Freundlich model ($mg_i^{1-1/n}\ L^{1/n}\ g_{dry\ sorbent}^{-1}$)
K_{Th}	Thomas rate constant (L h^{-1} mg^{-1})
m_s	Mass of the dry sorbent
MWW	Municipal wastewater
n_i	Inverse of the sorption intensity in the Freundlich model (−)
OC	Operating capacity of the sorbent ($mg_N\ g^{-1}_{dry\ sorbent}$)
v_s	Superficial velocity (m h^{-1})
WWTP	Wastewater treatment plant

Appendix A. Supplementary data

Supplementary data to this article can be found online at https://doi.org/10.1016/j.chemosphere.2024.143559.

Data availability

Research data underlying this manuscript have been published in the Zenodo Research Repository (https://doi.org/10.5281/zenodo.13798967).

References

Adam, M.R., Othman, M.H.D., Abu Samah, R., Puteh, M.H., Ismail, A.F., Mustafa, A., A Rahman, M., Jaafar, J., 2019. Current trends and future prospects of ammonia removal in wastewater: a comprehensive review on adsorptive membrane development. Sep. Purif. Technol. 213, 114–132. https://doi.org/10.1016/j.seppur.2018.12.030.

Arnoult, M., Perronnet, M., Autef, A., Rossignol, S., 2019. Geopolymer synthetized using reactive or unreactive aluminosilicate. understanding of reactive mixture. Mater. Chem. Phys. 237, 121837. https://doi.org/10.1016/j.matchemphys.2019.121837.

Asim, N., Alghoul, M., Mohammad, M., Amin, M.H., Akhtaruzzaman, M., Amin, N., Sopian, K., 2019. Emerging sustainable solutions for depollution: geopolymers. Construct. Build. Mater. 199, 540–548. https://doi.org/10.1016/j.conbuildmat.2018.12.043.

Beckinghausen, A., Odlare, M., Thorin, E., Schwede, S., 2020. From removal to recovery: an evaluation of nitrogen recovery techniques from wastewater. Appl. Energy 263, 114616. https://doi.org/10.1016/j.apenergy.2020.114616.

Bernal, M.P., Lopez-Real, J.M., 1993. Natural zeolites and sepiolite as ammonium and ammonia adsorbent materials. Bioresour. Technol. 43, 27–33. https://doi.org/10.1016/0960-8524(93)90078.

Canellas, J., Soares, A., Jefferson, B., 2019. Impact of presence and concentration of ionic species on regeneration efficacy of zeolites for ammonium removal. https://doi.org/10.26434/chemrxiv.9874754.v1.

Ciavarelli, R., Cappelletti, M., Fedi, S., Pinelli, D., Frascari, D., 2012. Chloroform aerobic cometabolism by butane-growing Rhodococcus aetherovorans BCP1 in continuous-flow biofilm reactors. Bioproc. Biosyst. Eng. 35, 667–681. https://doi.org/10.1007/s00449-011-0647-3.

Davidovits, J., 2008. Geopolymer Chemistry and Applications. Institute Geopolymer. St, Quentin Fr, 2011.

Duxson, P., Provis, J.L., Lukey, G.C., Mallicoat, S.W., Kriven, W.M., van Deventer, J.S.J., 2005. Understanding the relationship between geopolymer composition, microstructure and mechanical properties. Colloids Surf. A Physicochem. Eng. Asp. 269, 47–58. https://doi.org/10.1016/j.colsurfa.2005.06.060.

El-Eswed, B.I., 2019. Aluminosilicate inorganic polymers (geopolymers): emerging ion exchangers for removal of metal ions, in: inamuddin. In: Ahamed, M.I., Asiri, A.M. (Eds.), Applications of Ion Exchange Materials in the Environment. Springer International Publishing, Cham, pp. 65–93. https://doi.org/10.1007/978-3-030-10430-6_4.

Essaidi, N., Laou, L., Yotte, S., Ulmet, L., Rossignol, S., 2016. Comparative study of the various methods of preparation of silicate solution and its effect on the geopolymerization reaction. Results Phys. 6, 280–287. https://doi.org/10.1016/j.rinp.2016.05.006.

European Commission, 2019. Regulation - 2019/1009 - EN - EUR-Lex, 53, p. 37.

Foglia, A., Akyol, Ç., Frison, N., Katsou, E., Eusebi, A.L., Fatone, F., 2020. Long-term operation of a pilot-scale anaerobic membrane bioreactor (AnMBR) treating high salinity low loaded municipal wastewater in real environment. Sep. Purif. Technol. 236, 116279. https://doi.org/10.1016/j.seppur.2019.116279.

Franchin, G., Pesonen, J., Luukkonen, T., Bai, C., Scanferla, P., Botti, R., Carturan, S., Innocentini, M., Colombo, P., 2020. Removal of ammonium from wastewater with geopolymer sorbents fabricated via additive manufacturing. Mater. Des. 195, 109006. https://doi.org/10.1016/j.matdes.2020.109006.

Frascari, D., Bacca, A.E.M., Zama, F., Bertin, L., Fava, F., Pinelli, D., 2016. Olive mill wastewater valorisation through phenolic compounds adsorption in a continuous flow column. Chem. Eng. J. 283, 293–303. https://doi.org/10.1016/j.cej.2015.07.048.

Frascari, D., Molina Bacca, A.E., Wardenaar, T., Oertlé, E., Pinelli, D., 2019. Continuous flow adsorption of phenolic compounds from olive mill wastewater with resin XAD16N: life cycle assessment, cost–benefit analysis and process optimization. J. Chem. Technol. Biotechnol. 94, 1968–1981. https://doi.org/10.1002/jctb.5980.

Frascari, D., Zanaroli, G., Motaleb, M.A., Annen, G., Belguith, K., Borin, S., Choukr-Allah, R., Gibert, C., Jaouani, A., Kalogerakis, N., Karajeh, F., Ker Rault, P.A., Khadra, R., Kyriacou, S., Li, W.-T., Molle, B., Mulder, M., Oertlé, E., Ortega, C.V., 2018. Integrated technological and management solutions for wastewater treatment and efficient agricultural reuse in Egypt, Morocco, and Tunisia. Integr. Environ. Assess. Manag. 14, 447–462. https://doi.org/10.1002/ieam.4045.

Gagliano, E., Sgroi, M., Falciglia, P.P., Belviso, C., Cavalcante, F., Lettino, A., Vagliasindi, F.G.A., Roccaro, P., 2022. Removal of ammonium from wastewater by zeolite synthetized from volcanic ash: batch and column tests. J. Environ. Chem. Eng. 10, 107539. https://doi.org/10.1016/j.jece.2022.107539.

Gefenienė, A., Kauspėdienė, D., Snukiškis, J., 2006. Performance of sulphonic cation exchangers in the recovery of ammonium from basic and slight acidic solutions. J. Hazard Mater. 135, 180–187. https://doi.org/10.1016/j.jhazmat.2005.11.042.

Guida, S., Conzelmann, L., Remy, C., Vale, P., Jefferson, B., Soares, A., 2021. Resilience and life cycle assessment of ion exchange process for ammonium removal from municipal wastewater. Sci. Total Environ. 783, 146834. https://doi.org/10.1016/j.scitotenv.2021.146834.

Guida, S., Potter, C., Jefferson, B., Soares, A., 2020. Preparation and evaluation of zeolites for ammonium removal from municipal wastewater through ion exchange process. Sci. Rep. 10, 12426. https://doi.org/10.1038/s41598-020-69348-6.

Hedström, A., 2001. Ion exchange of ammonium in zeolites: a literature review. J. Environ. Eng. 127, 673–681. https://doi.org/10.1061/(ASCE)0733-9372(2001)127:8(673.

Hu, L., Yu, J., Luo, H., Wang, H., Xu, P., Zhang, Y., 2020. Simultaneous recovery of ammonium, potassium and magnesium from produced water by struvite precipitation. Chem. Eng. J. 382, 123001. https://doi.org/10.1016/j.cej.2019.123001.

Jorgensen, T.C., Weatherley, L.R., 2006. Continuous removal of ammonium ion by ion exchange in the presence of organic compounds in packed columns. J. Chem. Technol. Biotechnol. 81, 1151–1158. https://doi.org/10.1002/jctb.1481.
Jorgensen, T.C., Weatherley, L.R., 2003. Ammonia removal from wastewater by ion exchange in the presence of organic contaminants. Water Res. 37, 1723–1728. https://doi.org/10.1016/S0043-1354(02)00571-7.
Kithome, M., Paul, J.W., Lavkulich, L.M., Bomke, A.A., 1998. Kinetics of ammonium adsorption and desorption by the natural zeolite clinoptilolite. Soil Sci. Soc. Am. J. 62, 622–629. https://doi.org/10.2136/sssaj1998.03615995006200030011x.
Kroiss, H., Cao, Y., 2014. Energy considerations (chapter 12). In: Jenkins, D., Wanner, J. (Eds.), Activated Sludge – 100 Years and Counting. IWA Publishing. https://doi.org/10.2166/9781780404943.
Landi, E., Medri, V., Papa, E., Dedecek, J., Klein, P., Benito, P., Vaccari, A., 2013. Alkali-bonded ceramics with hierarchical tailored porosity. Appl. Clay Sci., Geopolymers: a new and smart way for a sustainable development 73, 56–64. https://doi.org/10.1016/j.clay.2012.09.027.
Langwaldt, J., 2008. Ammonium removal from water by eight natural zeolites: a comparative study. Sep. Sci. Technol. 43, 2166–2182. https://doi.org/10.1080/01496390802063937.
Laukkanen, J., Ojala, S., Luukkonen, T., Lassi, U., 2022. Effect of material age on the adsorption capacity of low-, medium-, and high-calcium alkali-activated materials. Appl. Surf. Sci. Adv. 12, 100345. https://doi.org/10.1016/j.apsadv.2022.100345.
Luukkonen, T., Heponiemi, A., Runtti, H., Pesonen, J., Yliniemi, J., Lassi, U., 2019. Application of alkali-activated materials for water and wastewater treatment: a review. Rev. Environ. Sci. Biotechnol. 18, 271–297. https://doi.org/10.1007/s11157-019-09494-0.
Luukkonen, T., Sarkkinen, M., Kemppainen, K., Rämö, J., Lassi, U., 2016. Metakaolin geopolymer characterization and application for ammonium removal from model solutions and landfill leachate. Appl. Clay Sci. 119, 266–276. https://doi.org/10.1016/j.clay.2015.10.027.
Luukkonen, T., Tolonen, E.-T., Runtti, H., Kemppainen, K., Perämäki, P., Rämö, J., Lassi, U., 2017. Optimization of the metakaolin geopolymer preparation for maximized ammonium adsorption capacity. J. Mater. Sci. 52, 9363–9376. https://doi.org/10.1007/s10853-017-1156-9.
Luukkonen, T., Věžníková, K., Tolonen, E.-T., Runtti, H., Yliniemi, J., Hu, T., Kemppainen, K., Lassi, U., 2018. Removal of ammonium from municipal wastewater with powdered and granulated metakaolin geopolymer. Environ. Technol. 39, 414–423. https://doi.org/10.1080/09593330.2017.1301572.
McCarty, P.L., Bae, J., Kim, J., 2011. Domestic wastewater treatment as a net energy producer–can this be achieved? Environ. Sci. Technol. 45, 7100–7106. https://doi.org/10.1021/es2014264.
Medri, V., Papa, E., Dedecek, J., Jirglova, H., Benito, P., Vaccari, A., Landi, E., 2013. Effect of metallic Si addition on polymerization degree of in situ foamed alkali-aluminosilicates. Ceram. Int. 39, 7657–7668. https://doi.org/10.1016/j.ceramint.2013.02.104.
Medri, V., Papa, E., Landi, E., Maggetti, C., Pinelli, D., Frascari, D., 2022. Ammonium removal and recovery from municipal wastewater by ion exchange using a metakaolin K-based geopolymer. Water Res. 225, 119203. https://doi.org/10.1016/j.watres.2022.119203.
Medri, V., Papa, E., Lizion, J., Landi, E., 2020a. Metakaolin-based geopolymer beads: production methods and characterization. J. Clean. Prod. 244, 118844. https://doi.org/10.1016/j.jclepro.2019.118844.
Medri, V., Papa, E., Mor, M., Vaccari, A., Natali Murri, A., Piotte, L., Melandri, C., Landi, E., 2020b. Mechanical strength and cationic dye adsorption ability of metakaolin-based geopolymer spheres. Appl. Clay Sci. 193, 105678. https://doi.org/10.1016/j.clay.2020.105678.
Novais, R.M., Seabra, M.P., Labrincha, J.A., 2017. Porous geopolymer spheres as novel pH buffering materials. J. Clean. Prod. 143, 1114–1122. https://doi.org/10.1016/j.jclepro.2016.12.008.
Panagiotopoulou, Ch, Kontori, E., Perraki, Th, Kakali, G., 2007. Dissolution of aluminosilicate minerals and by-products in alkaline media. J. Mater. Sci. 42, 2967–2973. https://doi.org/10.1007/s10853-006-0531-8.
Papa, E., Landi, E., Miccio, F., Medri, V., 2022. K2O-Metakaolin-Based geopolymer foams: production, porosity characterization and permeability test. Materials 15. https://doi.org/10.3390/ma15031008.
Papa, E., Medri, V., Amari, S., Manaud, J., Benito, P., Vaccari, A., Landi, E., 2018. Zeolite-geopolymer composite materials: production and characterization. J. Clean. Prod. 171, 76–84. https://doi.org/10.1016/j.jclepro.2017.09.270.
Papa, E., Medri, V., Benito, P., Vaccari, A., Bugani, S., Jaroszewicz, J., Swieszkowski, W., Landi, E., 2015. Synthesis of porous hierarchical geopolymer monoliths by ice-templating. Microporous Mesoporous Mater. 215, 206–214. https://doi.org/10.1016/j.micromeso.2015.05.043.
Pinelli, D., Bovina, S., Rubertelli, G., Martinelli, A., Guida, S., Soares, A., Frascari, D., 2022a. Regeneration and modelling of a phosphorous removal and recovery hybrid ion exchange resin after long term operation with municipal wastewater. Chemosphere 286, 131581. https://doi.org/10.1016/j.chemosphere.2021.131581.
Pinelli, D., Foglia, A., Fatone, F., Papa, E., Maggetti, C., Bovina, S., Frascari, D., 2022b. Ammonium recovery from municipal wastewater by ion exchange: development and application of a procedure for sorbent selection. J. Environ. Chem. Eng. 10, 108829. https://doi.org/10.1016/j.jece.2022.108829.
Pinelli, D., Molina Bacca, A.E., Kaushik, A., Basu, S., Nocentini, M., Bertin, L., Frascari, D., 2016. Batch and continuous flow adsorption of phenolic compounds from olive mill wastewater: a comparison between nonionic and ion exchange resins. Int. J. Chem. Eng. 2016, e9349627. https://doi.org/10.1155/2016/9349627.
Rasaki, S.A., Bingxue, Z., Guarecuco, R., Thomas, T., Minghui, Y., 2019. Geopolymer for use in heavy metals adsorption, and advanced oxidative processes: a critical review. J. Clean. Prod. 213, 42–58. https://doi.org/10.1016/j.jclepro.2018.12.145.
Rohm and Hass Company, 2005. Laboratory Procedures for Testing AmberlystTM and AmberliteTM ion exchange resins and adsorbents, pp. 1–12.
Sanguanpak, S., Wannagon, A., Saengam, C., Chiemchaisri, W., Chiemchaisri, C., 2021. Porous metakaolin-based geopolymer granules for removal of ammonium in aqueous solution and anaerobically pretreated piggery wastewater. J. Clean. Prod. 297, 126643. https://doi.org/10.1016/j.jclepro.2021.126643.
Siyal, A.A., Shamsuddin, M.R., Khan, M.I., Rabat, N.E., Zulfiqar, M., Man, Z., Siame, J., Azizli, K.A., 2018. A review on geopolymers as emerging materials for the adsorption of heavy metals and dyes. J. Environ. Manage. 224, 327–339. https://doi.org/10.1016/j.jenvman.2018.07.046.
Smil, Vaclav, 1992. Chapter 8 - agricultural energy costs: national analyses. In: Fluck, R. C. (Ed.), Energy in Farm Production, pp. 85–100.
Tchobanoglous, G., Burton, F.L., Stensel, H.D., Inc, M.&E., 2012. Wastewater Engineering: Treatment and Reuse. McGraw-Hill Education.
Vignoli, C.N., Bahé, J.M.C.F., Marques, M.R.C., 2015. Evaluation of ion exchange resins for removal and recuperation of ammonium–nitrogen generated by the evaporation of landfill leachate. Polym. Bull. 72, 3119–3134. https://doi.org/10.1007/s00289-015-1456-7.
Vocciante, M., De Folly D'Auris, A., Finocchi, A., Tagliabue, M., Bellettato, M., Ferrucci, A., Reverberi, A.P., Ferro, S., 2018. Adsorption of ammonium on clinoptilolite in presence of competing cations: investigation on groundwater remediation. J. Clean. Prod. 198, 480–487. https://doi.org/10.1016/j.jclepro.2018.07.025.
Wang, S., Peng, Y., 2010. Natural zeolites as effective adsorbents in water and wastewater treatment. Chem. Eng. J. 156, 11–24. https://doi.org/10.1016/j.cej.2009.10.029.
World Health Organization, 2006. Guidelines for the safe use of wastewater, excreta and greywater 2, 177–180.
Xiang, S., Liu, Y., Zhang, G., Ruan, R., Wang, Y., Wu, X., Zheng, H., Zhang, Q., Cao, L., 2020. New progress of ammonia recovery during ammonia nitrogen removal from various wastewaters. World J. Microbiol. Biotechnol. 36, 144. https://doi.org/10.1007/s11274-020-02921-3.
Xue, R., Donovan, A., Zhang, H., Ma, Y., Adams, C., Yang, J., Hua, B., Inniss, E., Eichholz, T., Shi, H., 2018. Simultaneous removal of ammonia and N-nitrosamine precursors from high ammonia water by zeolite and powdered activated carbon. J. Environ. Sci. 64, 82–91. https://doi.org/10.1016/j.jes.2017.02.010.
Ye, Y., Ngo, H.H., Guo, W., Liu, Y., Chang, S.W., Nguyen, D.D., Liang, H., Wang, J., 2018. A critical review on ammonium recovery from wastewater for sustainable wastewater management. Bioresour. Technol. 268, 749–758. https://doi.org/10.1016/j.biortech.2018.07.111.
Yu, R., Geng, J., Ren, H., Wang, Y., Xu, K., 2012. Combination of struvite pyrolysate recycling with mixed-base technology for removing ammonium from fertilizer wastewater. Bioresour. Technol. 124, 292–298. https://doi.org/10.1016/j.biortech.2012.08.015.
Yu, Y., Perumal, P., Corfe, I.J., Paul, T., Illikainen, M., Luukkonen, T., 2023. Combined granulation–alkali activation–direct foaming process: a novel route to porous geopolymer granules with enhanced adsorption properties. Mater. Des. 227, 111781. https://doi.org/10.1016/j.matdes.2023.111781.